Relativistic wave-induced splitting of the Langmuir mode in a magnetized plasma

J. Robiche* and J. M. Rax†

Laboratoire de Physique et Technologie des Plasmas, Ecole Polytechnique, Palaiseau, 91 128 Cedex, France

(Received 4 April 2007; revised manuscript received 17 October 2007; published 11 January 2008)

A relativistic effect that occurs in a magnetized plasma irradiated by a circularly polarized wave is identified and analyzed: the usual plasma frequency associated with longitudinal oscillations splits into two new frequencies. We set up a Hamiltonian description of the plasma dynamic in order to identify this effect that results from the coupling between the plasma oscillation and the transverse circular motion driven by both the magnetic and wave fields. Within the small oscillations approximation, we compute for right- and left-handed polarization the two characteristics frequencies of the electron oscillations as functions of the field and wave parameters. We also describe the electron trajectories in the wave, magnetic, and restoring plasma fields. This new class of oscillations is rotational and therefore radiate suggesting a method for the diagnostics of strong static magnetic field in laser-plasma experiments.

DOI: 10.1103/PhysRevE.77.016402 PACS number(s): 52.20.Dq, 52.25.Xz, 52.35.Fp

I. INTRODUCTION

The interaction between intense laser light and plasma is known to produce a plethora of nonlinear relativistic effects [1] such as fast particle productions [2–5], harmonics generation [6], or self-focussing. Among these effects, the generation by circularly polarized (CP) radiation of strong quasistatic axial magnetic field has attracted particular attention in the recent years [7–13]. This so-called inverse Faraday effect (IFE) that results from the absorption by the plasma of the angular momentum carried by a CP wave, was first predicted by Pitaevskii [14] and later rediscovered in plasmas by Deschamps *et al.* and Steiger and Wood [15]. IFE has been recently deeply revisited by Kostyukov *et al.* on the basis of a Hamiltonian analysis [7]. Measurement of such very large axial magnetic field, in the mega-Gauss range, generated by CP laser pulse at 10^{15} W cm^{-2} has been recently reported by Horovitz [16,17] and by Najmudin *et al.* [18] during interaction of CP laser pulse with an underdense plasma at ultrahigh intensity 10^{19} W cm^{-2}.

Here, our aim is to study the effect of such a strong axial static magnetic field on the bulk electrons collective dynamics. At the single particle level, the relativistic nonlinear electron orbit in a intense CP laser field has been thoroughly studied and is known to be the superposition of uniform drift motion and a circular motion [19]. When a homogeneous magnetic field is added, the motion remains near integrable. At the macroscopic level, in a magnetized plasma, electron plasma oscillation along the direction of a magnetic field are pure longitudinal wave which are not affected by the presence of the field [20]; the electrons motions are simple coherent oscillations with frequency ω_p. Perpendicular to the magnetic field, this frequency is shifted up to the upper hybrid frequency

$$\omega_{uh} = \sqrt{\omega_p^2 + \omega_c^2}, \tag{1}$$

where ω_c is the electron cyclotron frequency. The major results of this paper is that when CP transverse wave is added to the system, the electron oscillation frequency *along* the magnetic field line splits into two, hereafter so called upper ω_+ and lower ω_- frequencies, given by the formulas (for a right-hand circularly polarized wave)

$$\omega_\pm^2 = \frac{\omega_p^2}{2\gamma_0} + \frac{A^2\Omega\omega_p^2}{2\gamma_0^2(\gamma_0-\Omega)^2} + \frac{(\gamma_0-\Omega)^2}{2\gamma_0^2} \pm \frac{1}{2}\left[\left(\frac{\omega_p^2}{\gamma_0} + \frac{A^2\Omega\omega_p^2}{\gamma_0^2(\gamma_0-\Omega)^2} + \frac{(\gamma_0-\Omega)^2}{\gamma_0^2}\right)^2 - 4\left(\omega_p^2\frac{(\gamma_0-\Omega)^2}{\gamma_0^3} + \frac{A^2\Omega\omega_p^2}{\gamma_0^3(\gamma_0-\Omega)}\right)\right]^{1/2}, \tag{2}$$

$A=\frac{eE}{m_e c\omega}$, where E is the wave electric field, γ_0 a relativistic transverse energy defined later and Ω, the ratio of the cyclotron to the wave frequency.

This splitting of the Langmuir mode arises when a intense circularly polarized wave propagates in a magnetized plasma because the collective longitudinal oscillations driven by the restoring plasma field and the transverse circular motion driven by both the wave and magnetic fields are phase correlated. The purpose of this present work is to analyze within a Hamiltonian framework this complex collective response, to show up the splitting of the plasma frequency into two frequencies and to compute these two characteristics frequencies. The corresponding two frequencies rotational oscillation of the electrons in the wave, magnetic and restoring plasma fields is described. We also highlight the differences between right and left-handed polarization. We use the usual convention: for the right-hand circularly polarized mode (abbreviated as the *R*-mode in our paper), the wave fields rotate in the same direction as the electrons gyrate about the magnetic field lines. *L*-mode refers to the reversed situation.

This paper is organized as follows. In the next section, we set up the relativistic hamiltonian describing the electron oscillations embedded in an externally magnetized plasmas irradiated by an intense CP laser wave. In our study, the magnetic field in the plasma is supposed to be given; we do not address the issues of the self-generation of large magnetic field. Then to separate fast and slow dynamics and to regard

*robiche@greco2.polytechnique.fr
†rax@lptp.polytechnique.fr

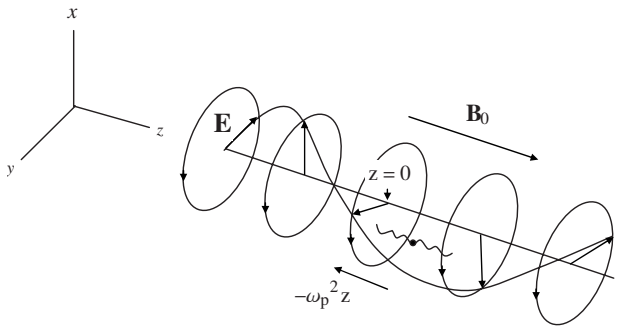

FIG. 1. The interaction of a relativistic electron with a static homogeneous magnetic field $\mathbf{B}_0=\Omega\mathbf{e}_z$ and a circularly polarized powerful laser wave.

the electron dynamics in the rest frame of the wave, we perform two successive canonical transformations. In Sec. III, based on the transformed Hamiltonian, we discover a fixed point function of the fields parameters and perform a local analysis in the harmonic approximation which yields to a set of two linear coupled oscillators describing, respectively, the electron dynamics in the longitudinal and in the transverse direction. Then, we calculate the characteristic frequencies of this collective electron dynamics and describe the electron orbits as a function of the field and wave parameters. In Sec. 4, we summarize and discuss our main results. Finally, last but not least, we mention the potential of this effect with regards to the diagnostics of strong static magnetic field in laser-plasma experiments. Throughout, in order to simplify this study, we will use the inverse of the wave frequency ω as a unit of time, c the speed of light as a unit of velocity, the electron charge e and mass m_e as units of charge and mass, respectively,

$$e = m_e = c = \omega = 1. \tag{3}$$

II. ANALYSIS OF THE ELECTRON DYNAMICS

Below we only perform the full computation for an R-wave. A summary of the derivation for the L-mode is given at the end of this section.

A. Hamiltonian

Let us consider the following fields in the plasma: a static homogeneous magnetic field $\mathbf{B}_0=\Omega\mathbf{e}_z$, the electromagnetic field of an R wave plus the electric field of a plasma wave (see Fig. 1). $(\mathbf{e}_x,\mathbf{e}_y,\mathbf{e}_z)$ is a Cartesian basis and Ω is the amplitude of the uniform magnetic field. The potential associated with the magnetic field reads

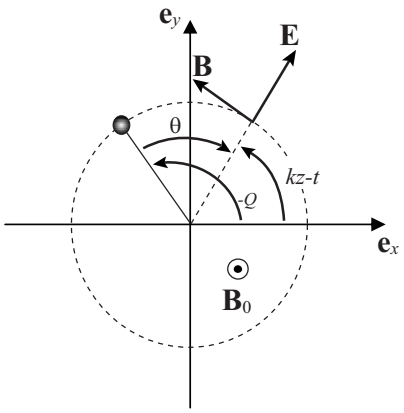

FIG. 2. Meaning of the variables.

$$\mathbf{A}_0 = \Omega x\mathbf{e}_y \tag{4}$$

and the one associated with the CP laser radiation reads

$$\mathbf{A}_\omega = A\cos(kz-t)\mathbf{e}_x - A\sin(kz-t)\mathbf{e}_y. \tag{5}$$

A and k are, respectively, the wave amplitude and the wave vector. We will refer to the axial or longitudinal direction as the direction along $\mathbf{e}_z$ and to the transverse direction to any direction in the plane $(\mathbf{e}_x,\mathbf{e}_y)$. The collective response is modeled by the electrostatic potential $\Phi(z)$ produced by the displacement of a slab of electrons from position $z=0$ to position z, i.e.,

$$\Phi(z) = \frac{1}{2}\omega_p^2 z^2. \tag{6}$$

In normalized units, the time-dependent relativistic hamiltonian describing the interaction between an electron and the potentials $\mathbf{A}(\mathbf{r},t)=\mathbf{A}_0(x)+\mathbf{A}_\omega(z,t)$ and $\Phi(z)$ reads

$$H(\mathbf{r},\mathbf{P},t) = \sqrt{1+[\mathbf{P}+\mathbf{A}(\mathbf{r},t)]^2} + \Phi(z). \tag{7}$$

Inserting Eqs. (4)–(6) into Eq. (7), we get the following Hamiltonian:

$$H(x,y,z,P_x,P_y,P_z,t) = \sqrt{1+P_z^2+[P_x+A\cos(kz-t)]^2+[P_y-A\sin(kz-t)+\Omega x]^2} + \frac{1}{2}\omega_p^2 z^2. \tag{8}$$

This Hamiltonian seems not to be integrable. Nevertheless, the characteristic of the collective electron dynamics can be obtained within the small oscillations approximations. In order to make further progress, two successive canonical transformations are performed. The first canonical change of variables $(x,y,z,P_x,P_y,P_z)\rightarrow(Q,Y,Z,P_Q,P_Y,P_Z)$ allow us to separate the fast dynamic occurring on the cyclotron time scale from the slow dynamic of the drift motion. It is given by the following generating function:

$$F_3(Q,Y,Z;P_x,P_y,P_z) = \frac{P_x P_y}{\Omega} - \frac{P_x^2 \tan Q}{2\Omega} - YP_y - ZP_z. \tag{9}$$

This transformation introduce the gyroangle Q, the transverse momentum P_Q, and the guiding center coordinates $(Y, -P_Y/\Omega)$. Other coordinates $z \equiv Z$ and $P_Z \equiv P_z$ are not modified by this transformation. Expressed with the set of variables (Q,Y,Z,P_Q,P_Y,P_Z), the transformed Hamiltonian (8) reads

$$H(Q,Z,P_Q,P_Z,t) = \sqrt{1 + A^2 + P_Z^2 + 2\Omega P_Q + 2A\sqrt{2\Omega P_Q}\cos[Q + (kZ - t)]} + \frac{1}{2}\omega_p^2 Z^2. \tag{10}$$

To analyze the electron dynamics in the rest frame of the wave, i.e., to eliminate the time dependence in Eq. (10), we perform the second canonical transformation $(Q,Y,Z,P_Q,P_Y,P_Z) \rightarrow (\theta,Y,Z,J,P_Y,P)$ given by

$$F_2(Q,Y,Z;J,P_Y,P;t) = J[Q + (kZ - t)] + YP_Y + ZP. \tag{11}$$

With this new set of variables (θ,Y,Z,J,P_Y,P), Hamiltonian (10) becomes autonomous

$$H(\theta,Z,J,P) = \sqrt{1 + A^2 + 2\Omega J + (P + kJ)^2 + 2A\sqrt{2\Omega J}\cos\theta} + \frac{1}{2}\omega_p^2 Z^2 - J. \tag{12}$$

These two transformations generate a new set of canonical variables related to the old set by

$$x = -\frac{P_Y}{\Omega} + \sqrt{\frac{2J}{\Omega}}\sin[\theta - (kZ - t)], \tag{13a}$$

$$y = Y - \sqrt{\frac{2J}{\Omega}}\cos[\theta - (kZ - t)], \tag{13b}$$

$$z = Z, \tag{13c}$$

$$P_x = \sqrt{2\Omega J}\cos[\theta - (kZ - t)], \tag{13d}$$

$$P_y = P_Y, \tag{13e}$$

$$P_z = P + kJ. \tag{13f}$$

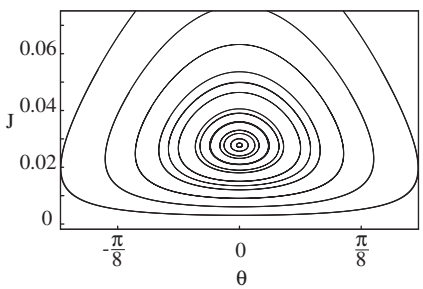

FIG. 3. Phase portrait in the (θ,J) plane showing for a R wave a fixed point located $\theta_0=0$ and $J_0=0.0268$. Plasma frequency is $\omega_p=0.1$.

These new variables have the following meaning (see Fig. 2), $\sqrt{\frac{2J}{\Omega}}$ is the gyration radius, θ the difference between the gyroangle and the wave phase, $\sqrt{2\Omega J}$ the transverse momentum. The linear momentum $P_z=P+kJ$ depends on the two canonical momentum P and J. Thus, the plasma oscillations along the magnetic field is correlated to the transverse electron dynamics driven by both the CP wave and the static field. As we stated in the Introduction, this coupling between the longitudinal and the transverse degree of freedoms induces a splitting of the plasma frequency into two frequencies ω_+ and ω_- which are function of the magnetic field Ω and of the CP laser amplitude A [see Eq. (2)]. Note that the old position z is equal to the new coordinate Z. Thus, the electron oscillations along the magnetic field correspond to the usual Langmuir oscillations at ω_p.

The generation through two successive CT of suitable canonical variables for the analysis of our system turns out to be fruitful. With these new canonical variables, the Hamiltonian (12) reveals the existence of an elliptic fixed point where the system is in stable equilibrium. This equilibrium leads us itself to analyze the electron collective motion within the small oscillations approximations. As a preliminary step, we determine below the characteristics of this fixed point.

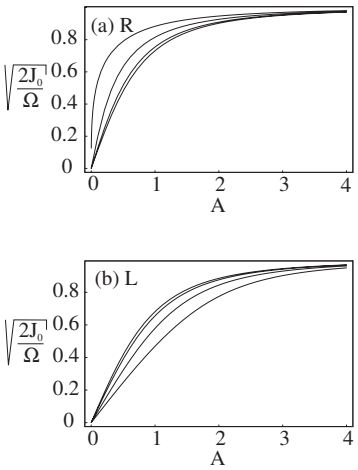

FIG. 4. Gyration radius at the fixed point for the R wave (a) (upper curve is for $\Omega=1$, lower curve is for $\Omega=0.1$) and the L wave (b) (upper curve is for $\Omega=0.1$, lower curve is for $\Omega=1$) as a function of the amplitude parameter A and for $\Omega=0.1,0.1,0.5$, and 1. This radius increases with the magnetic field for the R wave while decreases for the L wave (see Fig. 5).

B. Study of the fixed point

The phase portrait of Fig. 3 shows the results of the integration of the equation of motion associated with the Hamiltonian (12) for parameters $A=1$, $\Omega=0.1$, and $\omega_p=0.1$. This portrait reveals the existence of an elliptic fixed point located at $\theta_0=0$, $J_0=0.0267$ near which the dynamics is weakly non linear. In the following, the subscript 0 will refer to quantities evaluated at the fixed point. To find the location of this fixed point, we set to zero the time derivatives of the canonical coordinates

$$\left.\frac{\partial H}{\partial \theta}\right|_0 = 0, \tag{14a}$$

$$\left.\frac{\partial H}{\partial Z}\right|_0 = 0, \tag{14b}$$

$$\left.\frac{\partial H}{\partial P}\right|_0 = 0, \tag{14c}$$

$$\left.\frac{\partial H}{\partial J}\right|_0 = 0. \tag{14d}$$

The first three conditions yields

$$\theta_0 = 0 \bmod[\pi],\ Z_0 = 0 \quad \text{and} \quad P_0 + k\,J_0 = 0, \tag{15}$$

whereas the last conditions on $\partial H/\partial J$ yields to an implicit expression for J_0

$$\Omega + \frac{A\Omega\cos\theta_0}{\sqrt{2\Omega J_0}} - 1 = 0, \tag{16}$$

where

$$\gamma_0 = \sqrt{1 + A^2 + 2\Omega J_0 + 2A\sqrt{2\Omega J_0}\cos\theta_0} \tag{17}$$

must not be confused with the electron energy at the fixed point equals to $\gamma_0 - J_0$ [see Eq. (12) evaluated at the fixed point]. The angle θ_0 is multivalued, but as $\gamma_0 > \Omega$, condition (16) set the value θ_0 to 0, otherwise, this could never be satisfied. From Eq. (16) and for $\theta_0=0$ we obtain the following condition:

$$\sqrt{2\Omega J_0} = \frac{A\Omega}{\gamma_0 - \Omega} \tag{18}$$

which is a fourth order algebraic equation for the transverse momentum $X(A,\Omega) \equiv \sqrt{2\Omega J_0}$

$$X^4 + 2AX^3 + (1 + A^2 - \Omega^2)X^2 - 2A\Omega^2 X - \Omega^2 A^2 = 0. \tag{19}$$

A parametric study of the four roots show that there is only one positive real root for the relevant values of the parameters $1 \le A \le 10$ and $0 \le \Omega \le 1$. Inserting values (15) and the unique positive solution of Eq. (19) into Eq. (13), we obtain the electron orbit at the fixed point: a uniform circular motion with radius $\sqrt{\frac{2J_0}{\Omega}}$ and frequency equals the wave frequency $\omega=1$.

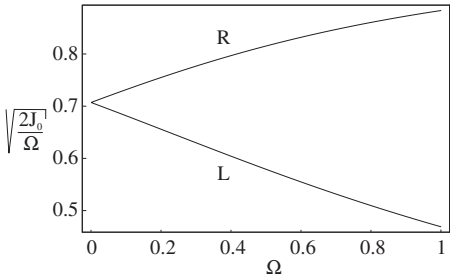

FIG. 5. Gyration radius at the fixed point for the R and L waves as a function of the magnetic field Ω for $A=1$. As $\Omega \to 0$, both value reduce to $A/\sqrt{1+A^2}$, the electron gyration radius in a CP wave.

The gyration radius [normalized to the wavelength according to our unit choice (3)] at the fixed point $\rho = \sqrt{\frac{2J_0}{\Omega}}$ is plotted on Fig. 4 for R-wave (a) and L-wave (b). We observe a weaker increase with A of ρ in the L-wave than in the R-wave. The asymptotic value of the gyration radius c/ω is reached once $A \sim 2$. The variation of the gyroradius with the magnetic field is depicted in Fig. 5 for both R and L wave. In the absence of magnetic field, the gyration radius of an electron in a CP wave is given by $A/\sqrt{1+A^2}$ [19]. When a homogeneous magnetic field is added, we observe that this radius increases with the magnetic field for a right-hand polarized wave while it decreases for the left-handed polarization. This original result is explained (and depicted on Fig. 6) by noting that for the R-wave, the centrifugal force points in the opposite direction than both the electric force and the Laplace force. On the contrary, for a L-wave, the Laplace force and the electric force point in opposite direction. It results that for the R-wave (respectively, L-wave), the required radius for which the forces balance is larger (respectively smaller) than the orbit radius of an electron in a CP wave.

C. Linearized dynamics

We now perform a local analysis and restrict ourselves to small oscillation. Within this regime, we expand the Hamiltonian (12) around the fixed point and keep only the quadratic terms

$$\begin{aligned} H(\theta,Z;J,P) \sim\ & \gamma_0 - J_0 + \frac{1}{2}\left.\frac{\partial^2 H}{\partial \theta^2}\right|_0 \theta^2 + \frac{1}{2}\left.\frac{\partial^2 H}{\partial Z^2}\right|_0 Z^2 \\ & + \frac{1}{2}\left.\frac{\partial^2 H}{\partial J^2}\right|_0 (J-J_0)^2 + \frac{1}{2}\left.\frac{\partial^2 H}{\partial P^2}\right|_0 (P-P_0)^2 \\ & + \left.\frac{\partial^2 H}{\partial J\,\partial P}\right|_0 (J-J_0)(P-P_0), \end{aligned} \tag{20}$$

where the term $\gamma_0 - J_0$ results from the injection of the fixed point coordinates (15) and (18) into the Hamiltonian (12). The explicit computation of the second derivatives at the fixed point is straightforward and yields the following expression:

$$\left.\frac{\partial^2 H}{\partial J^2}\right|_0 = \frac{k^2-1}{\gamma_0} - \frac{A\Omega^2}{\gamma_0 (2\Omega J_0)^{3/2}}, \tag{21a}$$

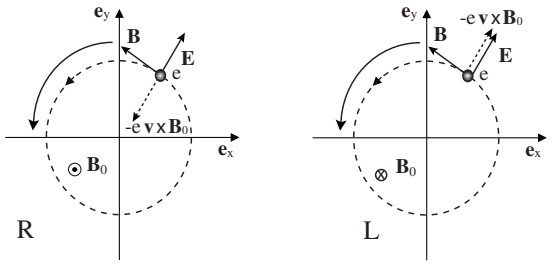

FIG. 6. The effect of the polarization on the orbit radius. For the L mode, the Laplace force $-e\mathbf{v}\times\mathbf{B}_0$ is directed in the outward direction as the centrifugal force $m_e\omega^2\mathbf{r}$. On the contrary, for the R mode, the Laplace force points in the inward direction.

$$\left.\frac{\partial^2 H}{\partial \theta^2}\right|_0 = -\frac{A^2\Omega}{\gamma_0(\gamma_0-\Omega)}, \tag{21b}$$

$$\left.\frac{\partial^2 H}{\partial Z^2}\right|_0 = \omega_p^2, \tag{21c}$$

$$\left.\frac{\partial^2 H}{\partial P^2}\right|_0 = \frac{1}{\gamma_0}, \tag{21d}$$

$$\left.\frac{\partial^2 H}{\partial J\,\partial P}\right|_0 = \frac{k}{\gamma_0}. \tag{21e}$$

The crossed derivative Eq. (21e), i.e., the coupling term into Hamiltonian (20), involves the wave vector k which is evaluated self-consistently by considering the wave equation with a source term given by the conduction current $-\omega_p^2\mathbf{V}_e$ induced by the electron motion at the fixed point

$$\left(\frac{\partial^2}{\partial t^2}-\nabla^2\right)\mathbf{A}_\omega = -\omega_p^2\mathbf{V}_e, \tag{22}$$

where $\mathbf{A}_\omega$ is given by Eq. (5) and $\mathbf{V}_e$ is the velocity of the electrons in the transverse direction. This velocity is obtained by taking the derivatives of the coordinates Eqs. (13a) and (13b) at the fixed point

$$\mathbf{V}_e = \frac{\sqrt{2\Omega J_0}}{\Omega}\begin{bmatrix}\cos(kz-t)\\ \sin(kz-t)\end{bmatrix} = \frac{A}{\gamma_0-\Omega}\begin{bmatrix}\cos(kz-t)\\ \sin(kz-t)\end{bmatrix}. \tag{23}$$

Inserting this current into the wave equation (22), we readily obtain the nonlinear dispersion relation

$$k^2 = 1-\frac{\omega_p^2}{\gamma_0(A,\Omega)-\Omega}. \tag{24}$$

This is apparently the result obtained by Akhiezer and Polovin [21] when they considered the propagation of a CP wave in a plasma. However, in the nonlinear formula (24),

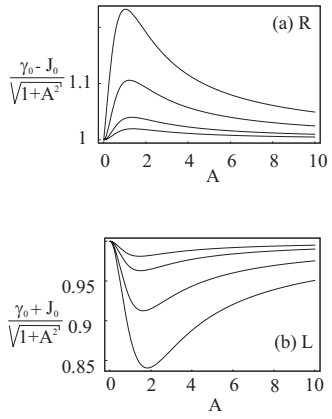

FIG. 7. Energy at the fixed point normalized to the electron mass in a CP wave $\gamma_0(A,0)=\sqrt{1+A^2}$ versus wave parameter A for magnetic field $\Omega=0.1$, 0.2, 0.5, and 1. (a) R wave (upper curve is for $\Omega=1$); (b) L wave (lower curve is for $\Omega=1$).

the quantity γ_0 is calculated self-consistently from Eq. (17) which depends on the magnetic field and on the wave amplitude.

In the small amplitude approximation, the motion equation derived from the Hamiltonian (20) yields to the following linear system of coupled harmonic oscillators

$$\frac{d\theta}{dt} = \left.\frac{\partial^2 H}{\partial J^2}\right|_0 (J-J_0) + \left.\frac{\partial^2 H}{\partial J\,\partial P}\right|_0 (P-P_0), \tag{25a}$$

$$\frac{dJ}{dt} = -\left.\frac{\partial^2 H}{\partial \theta^2}\right|_0 \theta, \tag{25b}$$

$$\frac{dZ}{dt} = \left.\frac{\partial^2 H}{\partial P^2}\right|_0 (P-P_0) + \left.\frac{\partial^2 H}{\partial J\,\partial P}\right|_0 (J-J_0), \tag{25c}$$

$$\frac{dP}{dt} = -\left.\frac{\partial^2 H}{\partial Z^2}\right|_0 Z. \tag{25d}$$

The standard independent normal mode techniques applied to the system (25) gives us the time evolution of the canonical variables as a linear superposition of harmonic oscillations

$$\theta(t) = \theta_+\sin(\omega_+ t)+\theta_-\sin(\omega_- t), \tag{26a}$$

$$J(t) = J_0 + J_+\sin(\omega_+ t)+J_-\sin(\omega_- t), \tag{26b}$$

$$Z(t) = Z_+\sin(\omega_+ t)+Z_-\sin(\omega_- t), \tag{26c}$$

$$P(t) = P_0 + P_+\sin(\omega_+ t)+P_-\sin(\omega_- t), \tag{26d}$$

with upper and lower frequency given by

$$\omega_\pm^R(A,\Omega,\omega_p) = \sqrt{\frac{B_R(A,\Omega,\omega_p)}{2}\pm\frac{\sqrt{B_R(A,\Omega,\omega_p)^2-4C_R(A,\Omega,\omega_p)}}{2}}. \tag{27}$$

The quantities $B_R(A,\Omega,\omega_p)$ and $C_R(A,\Omega,\omega_p)$ are given by

$$B_R(A,\Omega,\omega_p) = \left.\frac{\partial^2 H}{\partial J^2}\right|_0 \left.\frac{\partial^2 H}{\partial \theta^2}\right|_0 + \left.\frac{\partial^2 H}{\partial P^2}\right|_0 \left.\frac{\partial^2 H}{\partial Z^2}\right|_0, \tag{28a}$$

$$C_R(A,\Omega,\omega_p) = \left.\frac{\partial^2 H}{\partial J^2}\right|_0 \left.\frac{\partial^2 H}{\partial \theta^2}\right|_0 \left.\frac{\partial^2 H}{\partial P^2}\right|_0 \left.\frac{\partial^2 H}{\partial Z^2}\right|_0 - \left(\left.\frac{\partial^2 H}{\partial J\,\partial P}\right|_0\right)^2 \left.\frac{\partial^2 H}{\partial Z^2}\right|_0 \left.\frac{\partial^2 H}{\partial \theta^2}\right|_0 \tag{28b}$$

whose explicit analytical expression are obtained by substituting Eqs. (21) into Eq. (28)

$$B_R = \frac{A^2\Omega\omega_p^2}{\gamma_0^2(\gamma_0-\Omega)^2} + \frac{(\gamma_0-\Omega)^2}{\gamma_0^2} + \frac{\omega_p^2}{\gamma_0}, \tag{29a}$$

$$C_R = \omega_p^2\frac{(\gamma_0-\Omega)^2}{\gamma_0^3} + \frac{A^2\Omega\omega_p^2}{\gamma_0^3(\gamma_0-\Omega)}. \tag{29b}$$

The subscript R stands for the right-hand circular polarization. Equation (27) [or, equivalently, Eq. (2) stated in the Introduction] is one of the main result of this study and gives the two characteristic frequencies of the electron oscillation in a magnetized plasma irradiated by an intense CP R-wave as a function of the wave A, magnetic Ω, and plasma ω_p parameters. The corresponding results has been also obtained for the L-mode. This last task is summarized in the next section.

Before studying the result (27), let us consider the zero magnetic field limit. For $\Omega\to 0$ we get $\omega_+=1$ and $\omega_-=\omega_p/\gamma_0^{1/2}$. Moreover, the longitudinal collective motion is no longer coupled to the transverse motion and we have the classical oscillations $Z(t)=Z_-\sin(\omega_p/\gamma_0^{1/2}t)$. (As $\Omega\to 0$, second derivative of the Hamiltonian with respect to θ tends to zero, see Eq. (21b) so that J becomes a constant of the motion; therefore we have $J=J_0$ in Eq. (25c)). However, the transverse dynamics remains coupled to the longitudinal oscillations [see Eq. (21a)].

D. Left-handed polarization wave

We now briefly consider the case of a left-hand polarized light for which the electric field rotates in the opposite direction than the electrons and highlight the main difference with the R-wave case. Performing the same change of canonical variables, the transformed hamiltonian modeling the collective electron dynamics in a magnetized plasma irradiated by an intense L-wave reads

$$H(\theta,Z,J,P) = \sqrt{1+A^2+2\Omega J+(P-kJ)^2+2A\sqrt{2\Omega J}\cos\theta} + \frac{1}{2}\omega_p^2 Z^2 + J \tag{30}$$

which differs from Eq. (12) by the plus sign of the second term of the right hand side and by the sign in the coupling term $(P-kJ)$. The fixed point of the Hamiltonian (30) are given by

$$\theta_0 = \pi, \tag{31a}$$

$$P_0 = kJ_0, \tag{31b}$$

$$Z_0 = 0, \tag{31c}$$

$$\frac{A\Omega}{\sqrt{2\Omega J_0}} = \gamma_0 + \Omega, \tag{31d}$$

where the quantity γ_0 reads

$$\gamma_0 = \sqrt{1+A^2+2\Omega J_0 - 2A\sqrt{2\Omega J_0}}. \tag{32}$$

From Eq. (31d), the transverse momentum at the fixed point $X(A,\Omega)=\sqrt{2\Omega J_0}$ is the solution of the equation

$$X^4 - 2AX^3 + (1+A^2-\Omega^2)X^2 + 2A\Omega^2 X - \Omega^2 A^2 = 0 \tag{33}$$

which differs from Eq. (19) by the sign of the odd power coefficients. Performing the same step than to derive Eq. (24) from Eq. (22), we obtain the self-consistent wave vector k_L for the L wave

$$k_L^2 = 1 - \frac{\omega_p^2}{\gamma_0+\Omega}. \tag{34}$$

The characteristics frequencies $\omega_\pm$ for the L-mode are still given by Eq. (27) but with B_R and C_R replaced by B_L and C_L

$$B_L = -\frac{A^2\Omega\omega_p^2}{\gamma_0^2(\gamma_0+\Omega)^2} + \frac{(\gamma_0+\Omega)^2}{\gamma_0^2} + \frac{\omega_p^2}{\gamma_0}, \tag{35}$$

$$C_L = \omega_p^2\frac{(\gamma_0+\Omega)^2}{\gamma_0^3} - \frac{A^2\Omega\omega_p^2}{\gamma_0^3(\gamma_0+\Omega)} \tag{36}$$

with γ_0 given by Eq. (32) and $\sqrt{2\Omega J_0}$ given by the unique positive root of Eq. (33). The readers could think that B_L and C_L could be obtained from B_R and C_R by reversing the magnetic field $\Omega\to-\Omega$; however, Eqs. (32) and (33) differ from their counterparts Eqs. (17) and (19) so that the computation for the L-wave case must be also fully performed.

III. DISCUSSION AND CONCLUSION

Based on our Hamiltonian analysis of the small oscillations in a magnetized plasma irradiated by an intense CP wave, we discover that the classical Langmuir mode turns into a rotational two frequencies oscillations. The explicit expression for the two frequencies are given by Eq. (27) [or Eq. (2)]. Static magnetic field of the order of 100 mega-Gauss and more have been reported in many laser-plasma experiments [18] and confirmed by several fluid simulations. Thus, for Nd-glass laser operating at wavelength $\lambda=1.06\ \mu$m, the parameter $\Omega=\frac{\omega_c}{\omega}=10^{-2}\left[\frac{B}{\text{MGauss}}\right]$ is of the order of 1 and less. The following discussion aims to evaluate the presently reported effects for moderate relativistic intensity $A\sim 1$ and moderate strong field $\Omega\sim 1$ in an underdense plasma $\omega_p\sim 0.1$. The relevance of these effects with regards to the diagnostics of strong fields in plasma is argued at the end of the paper.

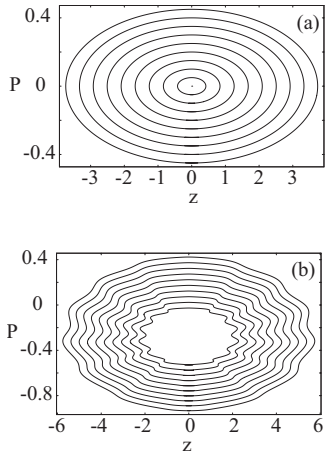

FIG. 8. Phase portrait in the (z,P) plane for $\Omega=0$ (a) and for a magnetized plasma $\Omega=0.1$ (b).

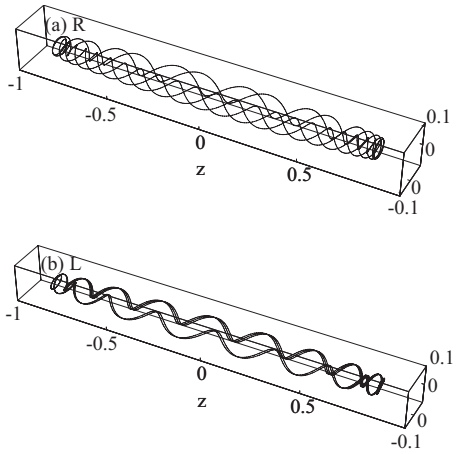

FIG. 9. Generic trajectory of an electron in the wave $(A=1)$, magnetic $(\Omega=0.1)$ and restoring plasma fields $(\omega_p=0.1)$ are shown in Fig. 9 for the R mode (a) and L mode (b). For both polarization, the initial conditions are $z_0=0$, $J=J_0$, and $P=P_0+0.1$ $[p_z(t=0)=0.1m_ec]$.

The electron energy at the equilibrium is given by γ_0-J_0 for the R-wave and by γ_0+J_0 for the L-wave. To bring out the influence of the magnetic field on the kinetic energy carried by the particles, we have normalized these energies to $\sqrt{1+A^2}$, the electron energy in a CP wave [19]. Figure 7 displays the variation of these energies with the magnetic field Ω for the R-wave (a) (the upper curve corresponds to $\Omega=1$) and the L wave (b) (the lower curve corresponds to $\Omega=1$). The effect of the magnetic field presents a sharp variation at subrelativistic energy and reaches in the R wave (respectively, L-wave) case a maximum (respectively, minimum) for wave parameters $A\sim 1$ (respectively, $A\sim 2$); at higher intensity, the wave field exceeds the magnetic field and the impact of Ω becomes less and less significant with respect to the carried energy.

Electron orbits in the phase plane (z,P) obtained with the numerical solutions of the motion equations associated to the exact Hamiltonian are shown in Fig. 8 for (a) $\Omega=0$ and (b) for $\Omega=0.1$. The wave parameter has value $A=1$, plasma frequency is $\omega_p=0.1$ and the transverses action J has been set for this instance to its equilibrium value J_0. The furthest out curve corresponds to the largest value of initial momentum P_0 which ranges from 0 to 5×10^{-1} in steps of 5×10^{-2}. When $\Omega=0$, the orbits present a single frequency periodic behavior and we found a angular frequency $\omega_p=0.083$ corresponding to plasma frequency with relativistic mass correction $\omega_p/(1+A^2)^{1/4}$. When magnetic field is added, however, the orbits present an obvious two frequencies periodic behavior; particles orbits are ellipsoidal-like curves-radially modulated by a high frequency component ω_+: the combination of a CP wave and of a magnetic field induce a splitting of the classical plasma frequency.

The generic trajectory of an electron in the wave, magnetic and restoring plasma fields are shown on Fig. 9 for R wave (a) and L wave (b). For both polarization, the initial conditions are $z_0=0$, $J=J_0$ and $P=P_0+0.1$ [thus $p_z(t=0)=0.1m_ec$]; initial angle is $\theta_0=0$ for the R mode and π for the L mode. These trajectories corresponds to oscillations in the longitudinal direction plus a gyration in the transverse plane.

The upper and lower frequencies Eqs. (27) are functions of the wave parameter A, of the magnetic field Ω and of the plasma density through ω_p. We present on Fig. 10, for the instance $\omega_p=0.1$, the variation of the lower frequency ω_- normalized to $\omega_p/(1+A^2)^{1/4}=\omega_p/\gamma_0(A,0)$ with A and Ω for the R wave (a) and L wave (b). When $\Omega=0$, we recover the classical value; electrons oscillates at the classical pulsation $\omega_-=\omega_p/\gamma_0^{1/2}$. For the R wave, the impact of the magnetic field is maximal at low intensity $A\lesssim 1$; at mildly relativistic energy $A\sim 1$, lower frequency ω_- is about few to 10% larger than ω_p/γ_0. However, when $A\gtrsim 2$, lower frequency ω_- do not depart from the plasma frequency with relativistic mass. The variations of the lower frequency for the L mode with A and Ω are weaker than for the R mode; the impact of the magnetic field reaches a maximum for relativistic amplitude $A\sim 1$.

The variation of the upper frequency ω_+ is shown in Fig. 11 for the R mode (a) and L mode (b). We observe that for both modes the lower the wave amplitude, the stronger the

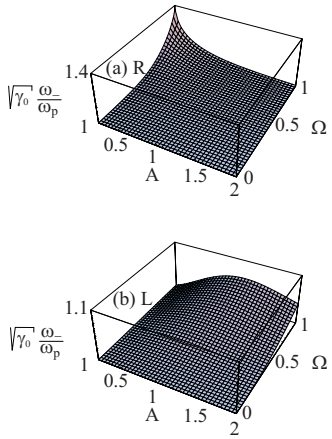

FIG. 10. (Color online) The lower frequency ω_- as a function of wave A and magnetic field parameter Ω. We have normalized ω_- to the plasma frequency with the relativistic mass $\omega_p/\gamma_0^{1/2}$. Plasma frequency is $\omega_p=0.1$.

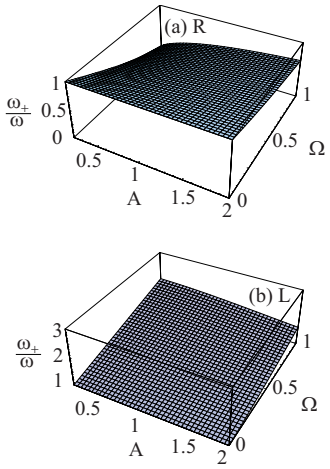

FIG. 11. (Color online) The upper frequency ω_+ normalized to ω as a function of wave and magnetic field parameter. Plasma frequency is $\omega_p=0.1$.

impact of the magnetic field. For $\Omega=0$, the upper frequency reduces to the wave frequency. For $A\to 0$, we have the expected results $\omega_+=1\mp\frac{\Omega}{\gamma_0}$.

Figure 12 shows the variation of the lower frequency normalized to $\omega_p/(1+A^2)^{1/4}$ with the magnetic field for $A=1$ (solid lines) and $A=2$ (dashed lines). For moderate intensity $A=1$, the lower frequency associated with the electron oscillations is practically the same for both polarization. The deviation from the value $\omega_p/(1+A^2)^{1/4}$ is 1% percent at $\Omega=0.1$ and reaches 6% at $\Omega=1$. This effect is weaker for $A=2$ as the fraction of the energy carried by the cyclotron motion decreases as the intensity increases.

Figures 13 and 14 show, respectively, the upper and lower frequency associated with the R and L mode for (a) $\omega_p=0.1$ and (b) $\omega_p=0.4$ as a function of the magnetic field. The wave parameter is $A=1$. For the R mode, upper and lower frequencies get closer when the magnetic field increases while depart from each others for the L mode.

We discovered that the electron oscillations in a magnetized plasma irradiated by a CP wave must be described by the combination of two motions: an oscillation $z(t)$ at main pulsation ω_- along the magnetic field modulated by a high frequency component at ω_+ plus a transverse motion given by

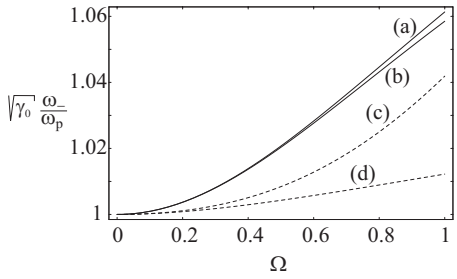

FIG. 12. The lower frequency ω_- normalized to the plasma frequency with relativistic mass $\omega_p/(1+A^2)^{1/4}$ ($\omega_p=0.1$) as a function of the magnetic field Ω for $A=1$ (solid lines) and $A=2$ (dashed lines). Labels (a) and (d) refer to the R mode; labels (b) and (c) refer to the L mode.

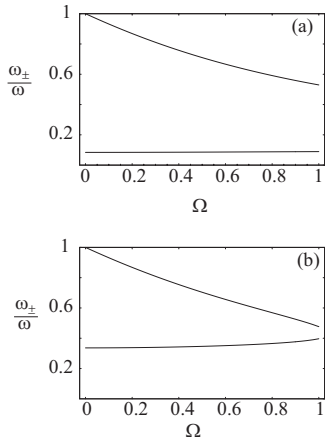

FIG. 13. The lower ω_- (lower curve) and upper frequency ω_+ (upper curve) normalized to the wave frequency ω versus the magnetic field Ω and for R-wave amplitude $A=1$. The upper figure (a) is for $\omega_p=0.1$ and the lower figure (b) for $\omega_p=0.4$.

$$x=\sqrt{\frac{2J(t)}{\Omega}}\sin[\theta(t)-kZ(t)\pm t], \tag{37a}$$

$$y=-\sqrt{\frac{2J(t)}{\Omega}}\cos[\theta(t)-kZ(t)\pm t], \tag{37b}$$

where $\theta(t)$ and $Z(t)$ and $J(t)$ are given by Eq. (26). For small oscillations, we have $J_\pm \ll J_0$ and therefore we can neglect

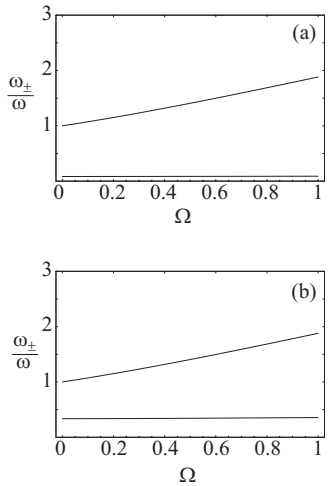

FIG. 14. The lower ω_- (lower curve) and upper frequency ω_+ (upper curve) normalized to the wave frequency ω versus the magnetic field Ω and for L-wave amplitude $A=1$. The upper figure (a) is for $\omega_p=0.1$ and the lower figure (b) for $\omega_p=0.4$.

the variation of the transverse action into Eq. (37). Being rotational, these two frequencies electron oscillations emits electromagnetic radiation whose spectrum shows peaks power centered on the frequencies ω, $\omega_+(\omega_c)$, and $\omega_-(\omega_c)$ and their harmonics. As such, the spectrum analysis of the power radiated by these new kind of oscillations could provide a promising tool for the diagnostic of strong magnetic field generated in laser-plasma experiments.

[1] G. A. Mourou, T. Tajima, and S. V. Bulanov, Rev. Mod. Phys. **78**, 309 (2006).

[2] C. Gahn, G. D. Tsakiris, A. Pukhov, J. Meyer-Ter-Vehn, G. Pretzler, P. Thirolf, D. Habs, and K. J. Witte, Phys. Rev. Lett. **83**, 4772 (1999).

[3] A. Pukhov, Z. M. Sheng, and J. Meyer-Ter-Vehn, Phys. Plasmas **6**, 2847 (1999).

[4] M. Key, Phys. Plasmas **5**, 1966 (1998).

[5] K. B. Wharton, S. P. Hatchett, S. C. Wilkis, M. H. Key, J. D. Moody, V. Yanovsky, A. A. Offenberger, B. A. Hammel, M. D. Perry, and G. Hoshi, Phys. Rev. Lett. **81**, 822 (1998).

[6] J.-M. Rax, J. Robiche, and I. Kostyukov, Phys. Plasmas **7**, 1026 (2000).

[7] I. Kostyukov, G. Shvets, N. J. Fisch, and J.-M. Rax, Phys. Plasmas **9**, 636 (2002).

[8] A. R. Bell, J. R. Davies, and S. M. Guerin, Phys. Rev. E **58**, 2471 (1998).

[9] V. I. Berezhiani, S. M. Mahajan, and N. L. Shatashvili, Phys. Rev. E **55**, 995 (1997).

[10] L. M. Gorbunov, P. Mora, and T. M. Antonsen Jr., Phys. Plasmas **4**, 4358 (1997).

[11] Z. M. Sheng and J. Meyer-ter-Vehn, Phys. Rev. E **54**, 1833 (1996).

[12] G. Shvets, N. J. Fisch, and J.-M. Rax, Phys. Rev. E **65**, 046403 (2002).

[13] T. Lehnert and L. di Menza, Phys. Rev. E **65**, 016414 (2001).

[14] L. P. Pitaevskii, Sov. Phys. JETP **12**, 1008 (1961).

[15] J. Deschamps, M. Fitaire, and M. Lagoute, Phys. Rev. Lett. **25**, 1330 (1970); A. D. Steiger and C. H. Woods, Phys. Rev. A **5**, 1467 (1972).

[16] Y. Horovitz, S. Eliezer, A. Ludmirsky, Z. Henis, E. Moshe, R. Shpitalnik, and B. Arad, Phys. Rev. Lett. **78**, 1707 (1997).

[17] Y. Horovitz *et al.*, Phys. Lett. A **246**, 329 (1998).

[18] Z. Najmudin *et al.*, Phys. Rev. Lett. **87**, 215004 (2001).

[19] J.-M. Rax, Phys. Fluids B **4**, 3963 (1992).

[20] A. I. Akkiezer *et al.*, *Collective Oscillations in a Plasma, Vol. 7 of International Series of Monographs in Natural Philosophy*. Pergamon, Oxford, 1967.

[21] A. I. Akhiezer and R. V. Polovin, Sov. Phys. JETP **3**, 696 (1956).